Investigating the Use of Fallout Radionuclides Beryllium-7 and Excess Lead-210 as Short-Term Stream Sediment Chronometers in the Agricultural Upper Midwest, USA

A THESIS
SUBMITTED TO THE FACULTY OF THE UNIVERSITY
OF MINNESOTA
BY

Ryan Hankins

IN PARTIAL FULFILLMENT OF THE REQUIREMENTS
FOR THE DEGREE OF
MASTER OF SCIENCE

Diana Karwan

2023

Acknowledgments

Many thanks to Dr. Diana Karwan, Dr. Lucy Rose, Dr. Ethan Pawlowski, and Dr. Brent Dalzell for all the hard work they did on this research before me. Each has asked research questions, designed sampling schemes, collected samples, or generated data to make this thesis possible.

Table of Contents

Chapter 1: Estimating Relative Ages of Suspended Stream Sediment using Beryllium-7 and Excess Lead-210 in an Agriculturally Polluted Watershed

Abstract

Sediment pollution from agricultural fields is a concern for surface water quality in the Upper Midwest even with best management practices in place to prevent field erosion. Legacy stores of previously eroded field sediment may build up in streams over time and lead to persistent water quality degradation. It is thus important to understand sediment settling and resuspension behavior in streams. For this project, I use the fallout radionuclides beryllium-7 (^{7}Be) and excess lead-210 ($^{210}Pb_{xs}$) to estimate the relative time since precipitation exposure, or "age", of suspended sediment at various points in a stream system in eastern Wisconsin on a storm event basis. The relative age of suspended sediment decreased along the downstream continuum as evidenced by increasing $^{7}Be/^{210}Pb_{xs}$ ratios. $^{7}Be/^{210}Pb_{xs}$ ratios ranged from 2.80 (+/- 0.11) to 4.16 (+/- 0.10) at the upstream site and 3.88 (+/- 0.25) to 7.32 (+/- 0.27) at the catchment outlet. The relative age of suspended sediment in an exposed drainage ditch was greater than that of a grassed waterway along the same field for two events. The $^{7}Be/^{210}Pb_{xs}$ ratio ranged from 2.10 (+/- 0.20) to 3.60 (+/- 0.31) in the exposed ditch and from 2.86 (+/- 0.23) to 5.78 (+/- 0.53) in the grassed waterway. There are two explanations for the increasing downstream trend in sediment ages. The first is that tile drainage may have delivered freshly tagged surface sediment to the outlet, increasing the relative freshness of sediment compared to the upstream sites that were unaffected by tile drainage. Secondly, ^{7}Be-dead sediment may have resuspended and been tagged with radionuclides while in the stream. It is likely that the suspended sediment in the grassed waterway was younger than in the exposed ditch because vegetation prevented scouring of the channel bed. FRN depositional

fluxes decreased in the winter such that the $^{7}Be/^{210}Pb_{xs}$ ratio of suspended sediment was greater than that of precipitation, causing inaccurate age calculations. FRN tagging of sediment in the Plum Creek watershed contrasted with comparable studies of other environments due to the landscape modifications of industrial agriculture and regional seasonal effects on FRN deposition. Future work using $^{7}Be/^{210}Pb_{xs}$ ratio to age sediment should incorporate robust precipitation sampling schemes and multiple lines of sediment source evidence to prevent misinterpretation of results.

Introduction

Excess sediment erosion from farmland is a major contributor to freshwater pollution in the agricultural Upper Midwest, USA (Wilken et al., 1982; Lambda et al., 2015). Sediment pollution in streams is of particular concern, as nutrients and metals easily sorb to fine grains and are transported to receiving waters or stored in the channel (Ballantine et al.,2009, Chen et al., 2016). Sediment also increases turbidity and blocks pores that facilitate hyporheic exchange (Shrivastava et al., 2020).

The downstream effects of fine sediment erosion present a need to understand fine-grain transport and deposition in agricultural landscapes and watersheds. Fine grains and associated nutrients like phosphorus may settle in the channel for months to years or wash out quickly over the course of a single storm event. Knowledge of sediment sources and relative ages in channels can help land managers evaluate the efficacy of best management practices (BMPs) used to control field erosion. If sediment moves quickly from fields to the outlet, the downstream effects of BMPs would be evident soon after their installment compared to if sediment resuspends many times before reaching the outlet. An extensive lag in fine-grain sediment delivery in agricultural regions could

build a legacy store of sediment and sediment-attached nutrients that contribute to eutrophication downstream long after BMPs are installed at field edges (Lannergård et al., 2020).

Fallout Radionuclides (FRNs) have been used to assess relative sediment ages in various stream systems (Dominik et al., 1987; Bonniwell et al., 1999; Le Gall et al., 2017; Gellis et al., 2017; Karwan et al., 2018;). Multiple definitions of sediment age exist in the literature (Muñoz-Arcos et al., 2022). Definitions of sediment age vary based on how one interprets the mechanism that starts a sediment chronometer or by the FRNs used. In stream systems, sediment age estimates are generally used to understand stream sediment sources or sediment transport processes. In this study, I define sediment age as the time since sediment has last been exposed to precipitation. Assuming precipitation primarily tags upland material with FRNs, this definition permits estimations of how much time has passed since sediment has washed from upland sites.

The FRNs beryllium-7 ($t_{1/2}$=53.12 d) and excess lead-210 ($t_{1/2}$= 22.3 y) are useful sediment tracers and chronometers (Matisoff et al., 2005). Beryllium-7 (^{7}Be) is produced in the stratosphere and upper troposphere by cosmic ray spallation of nitrogen and oxygen (Caillet et al., 2001). Lead-210 (^{210}Pb) is a daughter of the uranium-238 decay chain and is produced both in the soil and in the atmosphere by the decay of radon-222 gas (Ebaid and Khater, 2001). Atmospheric ^{210}Pb is considered "unsupported" or "excess" and is denoted as $^{210}Pb_{xs}$. ^{7}Be and $^{210}Pb_{xs}$ are often used together for sediment fingerprinting. Each wash from the atmosphere primarily as wet deposition. Once deposited to the surface, both adsorb strongly and irreversibly to fine particles under various environmental conditions (Pawlowski and Karwan, 2019). Assuming ^{7}Be and

$^{210}Pb_{xs}$ have similar delivery and sorption behaviors, their different half-lives allow for the use of $^{7}Be/^{210}Pb_{xs}$ to calculate the time since exposure to precipitation or the fraction of fresh sediment in suspension (Matisoff et al., 2005). The relatively short half-life of ^{7}Be makes it useful to estimate the short-term (days to weeks or months) relative ages of sediment. Precipitation tends only to interact with upland sites and not with stream channel banks or beds. Thus, the $^{7}Be/^{210}Pb_{xs}$ ratio can represent sediment source partitioning in watersheds. A $^{7}Be/^{210}Pb_{xs}$ ratio close to that of precipitation signifies the sediment is recently derived from the surface while lower FRN ratios represent channel bank and bed-derived sediment. Low FRN ratios may also indicate ditch and gully erosion or scouring of deeper soil in uplands (Matisoff et al., 2005).

While previous studies have characterized sediment ages along a downstream continuum, few have attempted this in highly modified catchments with land use dominated by industrial agriculture. Bonniwell et al., 1999 used a ^{7}Be, $^{210}Pb_{xs}$, and cesium-137 sediment tracing approach to calculate sediment ages along a downstream continuum in the mountainous Gold Fork River catchment in ID, USA. They observed sediment ages increasing along the downstream continuum, with ages ranging from 1.6 days near the headwaters to 106 days at the lowest elevations. Sediment ages may neatly increase downstream in a mountainous watershed, but these trends may differ in a relatively flat, clayey, tile-drained catchment. The research by Bonniwell et al. (1999) in a mountainous catchment is the reference point for explaining downstream trends in radionuclide activities, so I hypothesized that I would see the same increase in sediment age along the downstream continuum in Plum Creek. Barring other hydrological factors, it is plausible to think that sediment at upstream sites would more recently come from the

fields than the sediment at the outlet because studies by Fitzpatrick et al. (2019) and Rose and Karwan (2021) in this watershed observed this trend. The findings of these papers as they relate to the research of this thesis are further explained in the results section.

In this study, I use the $^{7}Be/^{210}Pb_{xs}$ ratio to characterize sediment ages on an event basis in an agriculturally polluted stream in eastern Wisconsin, USA. FRN analysis is paired with USGS stream gauge data on an event timescale, allowing for analysis of how FRN ratios in sediment relate to changes in stream discharge. The watershed in this project has also been the subject of sediment source partitioning studies (Fitzpatrick et al., 2019; Rose and Karwan, 2021). Hysteresis indices were calculated by Rose and Karwan (2021) to determine sediment pathways during the same storm events analyzed in this study, making it possible to compare spatial trends in suspended sediment $^{7}Be/^{210}Pb_{xs}$ ratios to another source partitioning technique.

Methods

Study Site

Plum Creek is a 92 km^2 tributary to the lower Fox River which feeds Lake Michigan in eastern Wisconsin (Fitzpatrick, 2019) (Fig. 1). The Fox River and lower Green Bay have been deemed areas of concern by the Great Lakes Restoration Initiative (GLRI) (U.S. EPA, 2012). GLRI projects respond to degraded water quality in the Great Lakes stemming from excess total suspended solids (TSS) and total phosphorus (G.L.I.T. Force, 2014). Plum Creek is a major contributor of sediment to the Fox River, producing an estimated 5,500 metric ton/yr of TSS (Cadmus, 2012). The watershed is near abundant dairy farm operations and is primarily covered by soybean and corn rotation cropland

while a deciduous forest encompasses much of the riparian zone (Wisconsin DNR, 2017). Plum Creek is characterized by silt loam and silty clay loam soil types (WSS, NRCS)

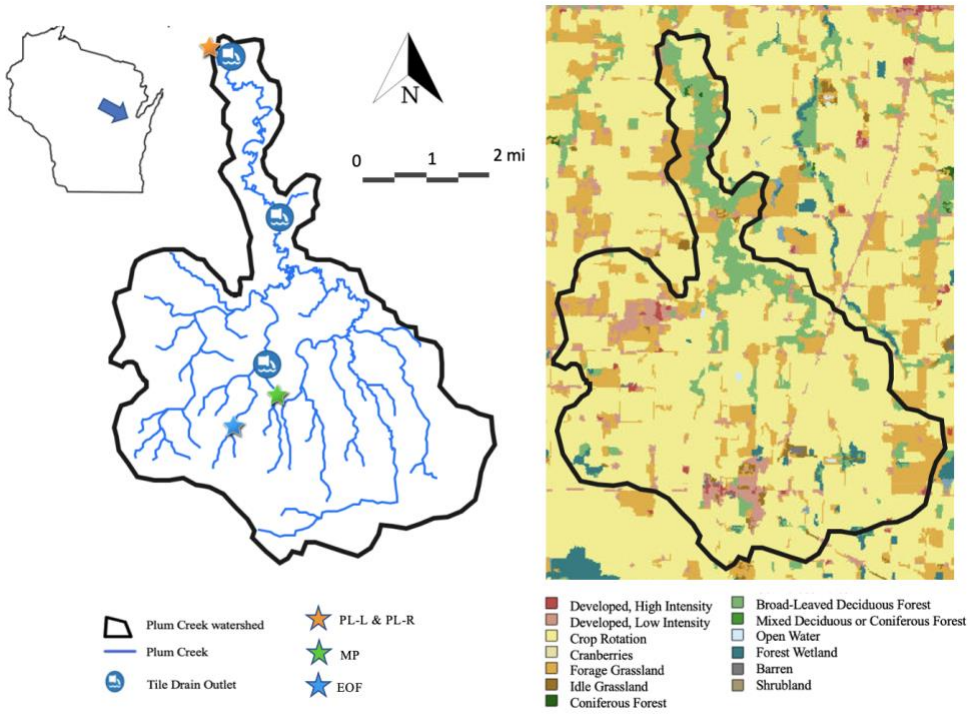

Figure 1: 2019 sampling locations and land use in the Plum Creek watershed. Land use information was retrieved from WDNR (2017).

Sampling Schemes

The sampling schemes differed in 2018 and 2019. For each year, passive samplers as described by Philips et al. (2000) were used to collect suspended sediment on a storm event or storm series basis. In 2018, both passive samplers were deployed in drainage ditches on different sides of a corn-soy rotation field in coordination with USGS and UW Green Bay Edge-of-Field studies (*Fig. 1: EOF Studies location*). One passive sampler deployed in the channel on the western edge of the field collected suspended sediment (SS) from a grassed waterway (West) and one passive sampler on the eastern edge collected SS from an exposed, unvegetated ditch (East). In 2019, passive samplers were

deployed in Plum Creek in a sequence downstream from one another below an edge-of-field site (*Fig.1*). One passive sampler was deployed at the edge-of-field site (EOF), one was deployed farther downstream at a mid-stream site (MP), and two were deployed at the outlet, one in the middle of the channel (PL-C) and another on the right side of the channel from the downstream-facing perspective (PL-R). The passive samplers at the outlet were near an operating USGS stream gauge that measures stream discharge continuously (USGS 04084911).

Passive samplers were deployed to sample suspended sediment after three 2018 and seven 2019 storm events between June and November. The duration of passive sampler deployment ranged from six to seven days in 2018 and four to thirty days in 2019. Some sampling periods included multiple storm events. Precipitation samples were collected at the EOF site in eight-inch funnels attached one-liter collection bottles, each washed with 5% HCl, and secured vertically to T-posts with O-rings. Precipitation samples were taken over the full duration of three events in 2018 and seven events in 2019 to account for between-storm variation in FRN deposition.

Gamma counting

Samples were gamma counted for ^{7}Be and $^{210}Pb_{xs}$ radioisotopes. ^{7}Be and ^{210}Pb were extracted from liquid samples (bulk precipitation) using exchange resins per Karwan et al. (2016). Suspended sediment, soils, or ion exchange resins from precipitation were sealed into 95.7 mL (6.38 cm diameter, 3.0 cm height) acrylic jars for analysis on high-purity germanium gamma-ray spectrometers (Mirion Canberra Model BEGe 3825 Broad Energy Germanium Detectors). Samples were counted for 24-48 hours within 108 days of collection for ^{7}Be and ^{210}Pb activity (Karwan et al., 2016). An

empty counting jar was used for blank calculation prior to determining peak areas. ^{7}Be peak area was measured for each sample based on multi-channel peaks and the neighboring 5 channels bracketing each peak as background and centered at 477 keV. $^{210}Pb_{xs}$ was calculated by subtracting the average of ^{214}Pb at 295 keV, ^{214}Pb at 352 keV, and ^{214}Bi at 609 keV from the total ^{210}Pb measured at 46.5 keV. This method assumes secular equilibrium within the jar that is counted, which can occur with the sample sealed in the jar for 21 days. Counting statistics for multi-channel peaks with multi-channel backgrounds were used to determine the one-sigma standard deviation of each peak as performed in Gilmore (2008). Minimum detectable activity (MDA) and counting limit were calculated for each sample as in Chapter 5 in Gilmore (2008). The efficiency of ^{7}Be at 477.7 keV was determined through interpolation between known peaks (Lead-210 at 46.5 keV, Americium-241 at 59.5 keV, Cadmium-109 at 88.0 keV, Cobalt-57 at 122.1 keV and Cesium-137 at 661.7 keV) in the mixed isotope standard (Eckert & Ziegler Analytics, Atlanta, GA).

Sediment Age Calculations

The ratios of ^{7}Be to $^{210}Pb_{xs}$ in precipitation and suspended sediment samples were used to calculate the time since the suspended sediment was exposed to precipitation per the methods of Matisoff et al. (2005). In this model, the relative age is computed and interpreted as the time since in contact with rainfall (Matisoff et al., 2005). Precipitation tags sediment with a particular ratio of $^{7}Be/^{210}Pb_{xs}$. Sediment is assumed to be tagged at upland sites that are exposed to precipitation while sediments from the channel bank, bed, and subsurface erosion are thought to be untagged (^{7}Be-dead), so it is possible to use the

FRN ratio to estimate the time since suspended sediment has washed from upland sites and into the stream channel.

$$t = \frac{-1}{\left(\lambda_{7_{Be}} - \lambda_{210_{Pb}}\right)} \ln\left(\frac{A}{B}\right) + \frac{1}{\left(\lambda_{7_{Be}} - \lambda_{210_{Pb}}\right)} \ln\left(\frac{A_o}{B_o}\right)$$

A = ^{7}Be activity concentration of SS

B = $^{210}Pb_{xs}$ activity concentration of SS

A_o = ^{7}Be activity concentration of precipitation

B_o = $^{210}Pb_{xs}$ activity concentration of precipitation

$\lambda_{7_{Be}}$= decay constant of ^{7}Be (0.01300 d^{-1})

$\lambda_{210_{Pb}}$= decay constant of ^{210}Pb ($8.05999 \cdot 10^{-5}$ d^{-1})

Equation 1: (Matisoff et al.,2005)

Eq.1 assumes that ^{7}Be and $^{210}Pb_{xs}$ are deposited in relatively consistent concentrations between rain events. If there is wide variability in the proportion of ^{7}Be to $^{210}Pb_{xs}$ concentrations in precipitation, sediment ages may be over or underestimated for some storms depending on how much FRN activity sediment has before it has been tagged. It is also impossible to distinguish between sediment that has aged because of decay and fresh sediment that has been diluted with ^{7}Be-dead sediment using this technique.

Results

Ten precipitation samples were measured at the EOF site for the 2018 and 2019 field seasons. ^{7}Be concentrations in precipitation collected at the EOF site for both years

ranged from 0 to 3.988 (+/- 0.05) $Bq \cdot kg^{-1}$ and $^{210}Pb_{xs}$ concentrations ranged from 0 to 0.799 (+/-0.54).

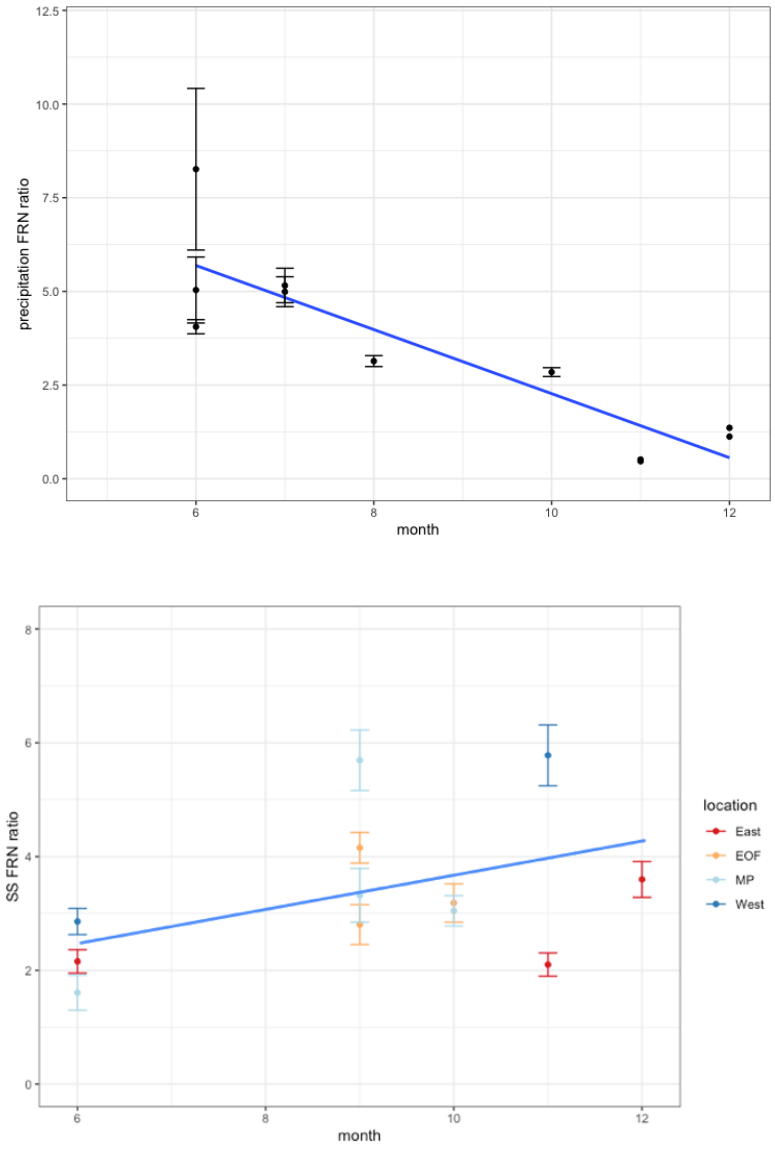

Figure 4a: (top) FRN ratios ($^{7}Be/^{210}Pb_{xs}$) of precipitation samples collected in 2018 and 2019 versus the month of collection at Plum Creek. Generally, FRN values were lower in the summer months than in winter, but there was no significant trend due to a small sample size.

Figure 4b: (bottom) FRN ratios of SS in 2018 and 2019 versus the month of collection and by location.

Seasonal variation in FRN ratios was more evident in precipitation than in SS among all samples (*Figs. 4a & b*). Summer showed much higher FRN ratios than late fall and early winter, consistent with the findings of other studies (Du et al.,2015, Karwan et al.,2018).

It was not possible to estimate accurate ages for several events in 2018 and 2019 due to greater FRN ratios in SS than in precipitation which resulted in negative relative age calculations. FRN ratios in precipitation tended to be less than those of SS in late autumn and winter (*Figs. 4a & b)*.

For the 2018 sampling period, the FRN ratios of SS in the exposed channel (East) ranged from 2.10 (+/- 0.20) to 3.60 (+/- 0.31) and from 2.86 (+/- 0.23) to 5.78 (+/-0.53) in the grassed waterway (West). The error for these ratios is the standard error of the activity concentration measurements by gamma ray spectroscopy of ^{7}Be and $^{210}Pb_{xs}$ in singular sediment samples propagated for the $^{7}Be/^{210}Pb_{xs}$ ratio of each sample. For both events with SS measured at both sites in 2018, the grassed waterway had a greater FRN ratio than the exposed channel, as shown in *Fig. 2.*

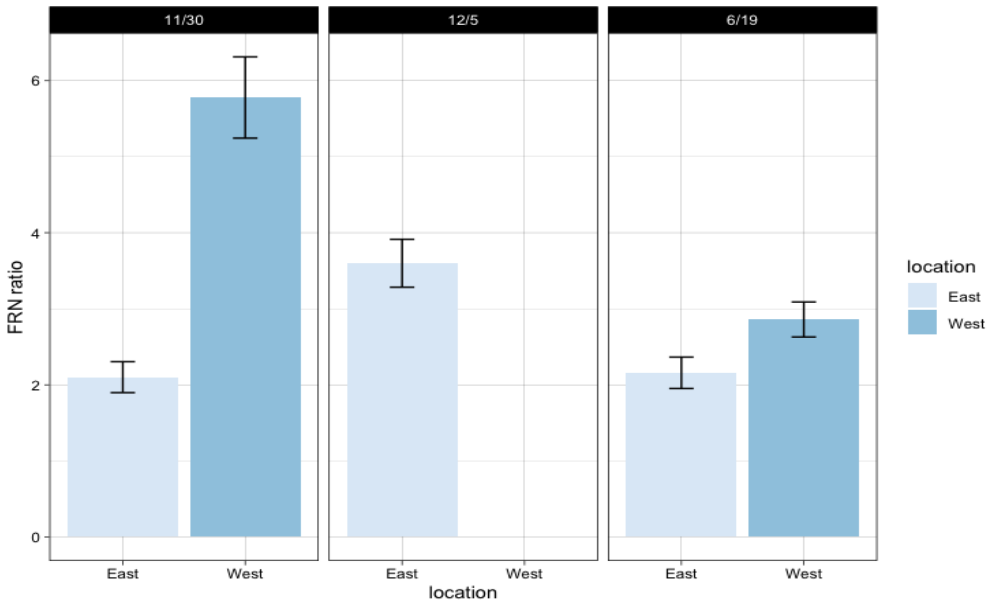

Figure 2: FRN ratios of SS at the East (unvegetated channel) and West (grassed waterway) sites in 2018. A SS sample could not be retrieved from the West site on 12/5. Error bars represent the propagated standard error of the measured ^{7}Be activity concentration over the $^{210}Pb_{xs}$ concentration.

It was only possible to estimate the relative sediment age for one date in 2018. On 6/19/18, the relative age of SS was estimated to be 48.856 (±0.142) days at the East site and 27.08 (±0.127) days at the West site. SS ages could not be calculated for other dates in 2018 because the FRN ratios of precipitation were measured to be lower than those of SS. This occurred for the 11/30/18 and 12/05/18 sampling dates.

The nested sampling scheme performed in 2019 showed increasing trends of FRN ratios along the downstream continuum for events where samples could be collected from multiple sites along the reach (*Fig. 3*). Samples for site locations are missing for July, August, and September dates because passive samplers at some sites were either buried by sediment from storms or not enough sediment was captured to analyze for FRN

concentrations. The sampling locations at the outlet (PL-C and PL-R) had greater FRN ratios than the upstream sites (MP and EOF) for both events where upstream and downstream sites were measured.

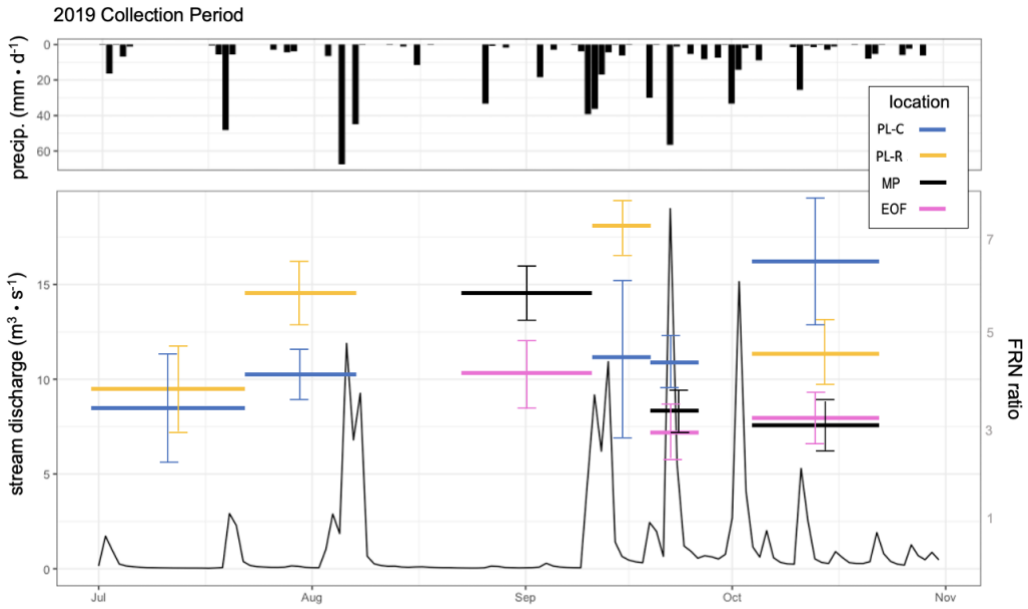

Figure 3: Total daily precipitation, stream discharge, and $^{7}Be/^{210}Pb_{xs}$ (FRN ratio) of suspended sediment for the 2019 collection period. The horizontal length of the colored bars indicates the passive sampler deployment periods, and the date each bar ends is the collection date for that deployment period.

Precipitation was collected for two events in 2019, however, SS ages could only be calculated for one 2019 event due to a lack of precipitation sampling and a lower FRN ratio in precipitation than in SS for the 10/23 sampling date. The age of SS was estimated to be 24.07 (±0.43) days at PL-C and 32.36 (±0.34) days at PL-R (*Table 1*.). Ages were not able to be calculated on 10/23/19 because the FRN ratios of precipitation were again lower than those of SS.

Sample Date	location	^{7}Be (Bq · kg^{-1})	$^{210}Pb_{xs}$ (Bq · kg^{-1})	FRN ratio	age (days)	Hysteresis Index
6/27/19	MP	45.214 (±2.442)	28.113 (±3.886)	1.608 (±0.309)	NA	-0.20
7/22/19	PL-C	116.244 (±2.278)	30.753 (±9.857)	3.780 (±1.286)	24.07 (±0.43)	-0.03
	PL-R	119.691 (±1.917)	76.713 (±-0.911)	3.396 (±0.846)	32.36 (±0.34)	-0.03
8/9/19	PL-C	66.603 (±0.945)	16.125 (±1.708)	4.130 (±0.496)	NA	0.49
	PL-R	76.713 (±0.911)	13.327 (±1.61)	5.756 (±0.764)	NA	0.49
9/13/19	MP	119.333 (±1.256)	20.962 (±1.732)	5.693 (±0.530)	NA	-0.2
9/25/19	MP	85.326 (±2.176)	25.706 (±3.008)	3.319 (±0.473)	NA	0.43

Table 1: FRN analysis results are compared with hysteresis indices measured by Rose & Karwan (2021) for the same events and locations.

Rose & Karwan (2021) computed hysteresis indices of TSS at Plum Creek during the same timeframe as some collections were made for this study (*Table 1*). Clockwise hysteresis (hysteresis index > 1) indicates near and in-channel sediment sources, while anticlockwise hysteresis (hysteresis index < 1) signifies a lag in sediment delivery that can be associated with sediment from upland sources. FRN ratios only vary slightly and are within the bounds of error between events with different hysteresis directionality at the same sites. The hysteresis index does not seem to be a strong indicator of FRN ratios, meaning the apparent relative age of sediment doesn't change much with sediment source differences in Plum Creek.

No significant relationship was evident between the FRN ratio of SS and the total stream discharge or peak stream discharge over the sampling duration.

Discussion

There was an increasing trend of FRN ratios along the downstream continuum in 2019. Under the analysis model of Matisoff et al. (2005), this would indicate relatively younger sediments downstream in the watershed. The assumptions of relative stream sediment contributions based on FRN ratios using the Matisoff et al. (2005) conceptual framework do not align with the conclusions of previous sediment fingerprinting work in the same watershed. Fitzpatrick et al. (2019) found that on an annual basis in the Plum Creek watershed, most suspended sediments at the channel outlet derive from stream banks, gullies, and ditches, while a small portion comes from forests and cropland. Cropland made up a larger portion of the source of stream sediment in the upper reaches, while downstream sediment was found to derive primarily from bank contribution. A study by Rose and Karwan (2021) of sediment concentration-discharge relationships in the Plum Creek watershed during the same sampling periods as this study found prevalent anti-clockwise hysteresis in the upper reaches, indicating distal sediment sources, and more clockwise hysteresis near the outlet, indicating near and in-channel sources. The Matisoff et al. (2005) model assumes that young sediment ages represent upland sediment sources and old sediment represents near-channel or subsurface sources. Under these assumptions, the increasing FRN ratios along the downstream continuum seem to disagree with the sediment source fingerprinting studies of Fitzpatrick et al.(2019) and Rose and Karwan (2021). Thus, ^{7}Be enriched sediment at the outlet cannot be assumed to mostly reflect overland flow contribution to SS but instead reflect tagging by other means.

There are two primary explanations for the increasing downstream trend in ^{7}Be-enriched sediments. First, this trend may be explained by the PL sites' positions relative to tile drainage. As depicted in Fig 1., the sampling sites near the stream outlet were downstream from three tile drain outlets. Eguchi et al.(2010) found that mobile soil particles from tile drainage waters tended to derive from the upper portion of the soil, resulting in higher ^{7}Be readings of sediment coming from tile drains. Karwan and Williamson (in prep) have found measurable ^{7}Be in tile drain effluent when tile lines have unintended surface connections (Karwan in prep). Tile drainage may have contributed to suspended sediment near the outlet, resulting in higher ^{7}Be activities in SS at the PL site than at the two upstream sites. Mobile soil particles collected at the outlet may have derived from upland topsoil but reached the outlet via tile drainage rather than overland flow. A second explanation is that in-stream tagging of re-suspended channel sediments could have occurred. In some cases, direct-channel precipitation can influence FRN activities of suspended sediment (Karwan et al., 2018). Precipitation may have contributed high enough concentrations of FRNs to the stream water that sediment was tagged while in suspension. FRNs sorb more to sediment the longer they are in contact with one another (Pawlowski and Karwan, 2019). It is possible that FRNs adsorbed to SS as they traveled through the channel and became highly concentrated with FRNs by the time they reached the outlet.

Analysis of the 2018 paired-field samples showed storm events resulted in lower FRN ratios in the unvegetated control channel than in the grassed waterway channel. This may indicate that vegetation in the grassed waterway prevented older sediment from being scoured from the ditch during the storm event, resulting in higher SS FRN ratios in

the collector. Sediment flux data may have helped to further corroborate this idea if less sediment was captured by the passive collector at the West site, but no such data were recorded. Meanwhile, the exposed channel yielded SS with lower FRN ratios. In the exposed channel, a lack of vegetative cover may have permitted older sediment to be more easily scoured from the channel bed, yielding relatively lower FRN ratios in captured SS.

Seasonal variation in the deposition of FRNs was evident over the course of this study, as in previous studies (Baskaran et al., 1995; Landis et al., 2022). FRN ratios in precipitation were consistently higher in the summer and early fall than in the late fall and winter. The increase in ^{7}Be concentrations in precipitation in summer may be explained by large-scale atmospheric mixing in the summer that has been found to increase ^{7}Be scavenging by clouds (Dueñas et al.,2001; McNeary & Baskaran, 2003). Conversely, there were not any remarkable seasonal trends in SS FRN ratios. SS FRN ratios may not have shown seasonal variation akin to precipitation because frequent retagging of sediment by storms in winter may have maintained higher SS FRN ratios compared to the FRN ratios of precipitation that reduce during the colder months. The most unexpected finding was that some storm events in the late fall and early winter showed lower FRN activities in precipitation than in sediment at both the East and West EOF sites in 2018. This may be a result of the high variability of ^{7}Be deposition between storms and the comparatively low ^{7}Be depositional flux in the winter. I explore this variation extensively in the second chapter of this thesis. It is also possible that ^{7}Be hadn't fully decayed in surface material before it was retagged by precipitation. Reserve

^{7}Be activity in SS from preceding events may have been compounded by precipitation that was comparatively low in ^{7}Be concentrations.

The inability to consistently sample at all locations for every event was one limitation of this study. Passive collectors at every location but the East EOF site were periodically buried by sediment mobilized during storms or did not collect enough SS for gamma counting. These circumstances prevented SS collections at some sites for several storms in 2018 and 2019. There were also challenges in retrieving precipitation samples for many events because of the long travel time to the field site and the variability of weather patterns. These problems prohibited the generation of sample sizes sufficient to calculate regressive relationships and impacted the consistency of collections. In the future, rainfall collections should be performed around a wide range of the study area to account for the high variability of FRN deposition.

Another limitation of this study is that it is impossible to distinguish between fresh sediment and resuspended sediment tagged within the stream channel using FRN tracers alone (Matisoff et al., 2005). This may have caused false indications of sediment freshness if resuspended channel sediment was tagged with FRNs while in the stream.

Conclusions

The results of this study showed an increase in relative sediment freshness along the downstream continuum after storm events in Plum Creek. This runs counter to previous studies, particularly those developed in mountainous watersheds. The downstream increase in SS FRN ratios could be explained by tile drainage delivery of FRN-enriched topsoil to the stream outlet or by in-stream tagging of re-suspended sediments by precipitation. Ultimately, estimating sediment ages in the stream channel

benefitted by pairing FRN analysis with multiple lines of evidence related to sediment source partitioning. With FRNs alone, sediment sources may have been deduced incorrectly due to the complexity tile drainage adds to this catchment's hydrology. FRN analysis further provided evidence that the grassed drainage ditch prevented channel scouring during storm events, showing the BMP effectively slowed the delivery of older sediment to stream channels. I also found that low FRN depositional fluxes in the winter and late fall could result in higher FRN ratios in SS than in precipitation, causing inaccurate estimates of sediment ages.

Works Cited

Ballantine, D. J., et al. "The content and storage of phosphorus in fine-grained channel bed sediment in contrasting lowland agricultural catchments in the UK." *Geoderma* 151.3-4 (2009): 141-149.

Baskaran, M. "A search for the seasonal variability on the depositional fluxes of 7Be and 210Pb." *Journal of Geophysical Research: Atmospheres* 100.D2 (1995): 2833-2840.

Bonniwell, Everett C., Gerald Matisoff, and Peter J. Whiting. "Determining the times and distances of particle transit in a mountain stream using fallout radionuclides." *Geomorphology* 27.1-2 (1999): 75-92.

Cadmus. 2012. Total maximum daily load and watershed management plan for total phosphorus and total suspended solids in the lower Fox River Basin and Lower Green Bay. The Cadmus Group report.

Caillet, Stéphane, et al. "Factors controlling 7Be and 210Pb atmospheric deposition as revealed by sampling individual rain events in the region of Geneva, Switzerland." *Journal of Environmental Radioactivity* 53.2 (2001): 241-256.

Chen, Yueh-Min, et al. "Relationship between heavy metal contents and clay mineral properties in surface sediments: Implications for metal pollution assessment." *Continental Shelf Research* 124 (2016): 125-133.

Dominik, J., D. Burrus, and J-P. Vernet. "Transport of the environmental radionuclides in an alpine watershed." *Earth and Planetary Science Letters* 84.2-3 (1987): 165-180.

Du, Juan, et al. "Temporal variations of atmospheric depositional fluxes of 7Be and 210Pb over 8 years (2006–2013) at Shanghai, China, and synthesis of global fallout data." *Journal of Geophysical Research: Atmospheres* 120.9 (2015): 4323-4339.

Dueñas, C., et al. "Atmospheric deposition of 7Be at a coastal Mediterranean station." Journal of Geophysical Research: Atmospheres 106.D24 (2001): 34059-34065.

Ebaid, Y. Y., and A. E. M. Khater. "Determination of 210 Pb in environmental samples." *Journal of Radioanalytical and Nuclear Chemistry* 270.3 (2006): 609-619.

Eguchi A, Sadao, et al. "Cosmogenic, anthropogenic, and airborne radionuclides for tracing the mobile soilparticles in a tile-drained heavy clay soil." *19th World Congress of Soil Science*. 2010.

Fitzpatrick, Faith A., et al. "Stream corridor sources of suspended sediment and phosphorus from an agricultural tributary to the Great Lakes." *SEDHYD 2019 Conference*. Vol. 4. 2019.

Gellis, Allen C., Christopher C. Fuller, and Peter C. Van Metre. "Sources and ages of fine grained sediment to streams using fallout radionuclides in the Midwestern United States." *Journal of Environmental Management* 194 (2017): 73-85.

Great Lakes Interagency Task Force. "Great Lakes restoration initiative action plan II." *Great Lakes Restoration http://www. greatlakesrestoration. us/actionplan/pdfs/glri-action-plan-2. pdf (accessed 11 Jan 2018)* (2014).

Karwan, Diana L., et al. "Direct channel precipitation and storm characteristics influence short term fallout radionuclide assessment of sediment source." *Water Resources Research* 54.7 (2018): 4579-4594.

Lamba, Jasmeet, et al. "Sources of fine sediment stored in agricultural lowland streams, Midwest, USA." *Geomorphology* 236 (2015): 44-53.

Landis, Joshua David, et al. "Patterns and Processes in Aerosol Bulk Deposition: Insights from a 9-year Study of 7Be, 210Pb, Sulfate and Major/Trace Elements." *Authorea Preprints* (2022).

Lannergård, Emma E., et al. "New insights into legacy phosphorus from fractionation of streambed sediment." *Journal of Geophysical Research: Biogeosciences* 125.9 (2020):e2020JG005763.

Le Gall, Marion, et al. "Investigating the temporal dynamics of suspended sediment during flood events with 7Be and 210Pbxs measurements in a drained lowland catchment." *Scientific Reports* 7.1 (2017): 42099.

Muñoz-Arcos, E., et al. "Understanding the complexity of sediment residence time in rivers: Application of Fallout Radionuclides (FRNs)." *Earth-Science Reviews* (2022): 104188.

Pawlowski, Ethan D., and Diana L. Karwan. "Assessment of lead and beryllium sorption to exposed stream channel sediment under varying freshwater channel conditions." *Journal of Soils and Sediments* 19 (2019): 3397-3410.

Rose, Lucy A., and Diana L. Karwan. "Stormflow concentration–discharge dynamics of suspended sediment and dissolved phosphorus in an agricultural watershed." *Hydrological Processes* 35.12 (2021): e14455.

Shrivastava, Shivansh, Michael J. Stewardson, and Meenakshi Arora. "Distribution of clay-sized sediments in streambeds and influence of fine sediment clogging on hyporheic exchange." *Hydrological Processes* 34.26 (2020): 5674-5685.

Soil Survey Staff, Natural Resources Conservation Service, United States Department of Agriculture. Web Soil Survey. Available online at http://websoilsurvey.nrcs.usda.gov/.

United States Environmental Protection Agency. “Lower Green Bay/Fox River AOC.” *EPA*, 12 Oct. 2022, www.epa.gov/great-lakes-aocs/lower-green-bayfox-river-aoc.

Wilkin, Donovan C., and Susan J. Hebel. "Erosion, redeposition, and delivery of sediment to Midwestern streams." *Water Resources Research* 18.4 (1982): 1278 -1282.

Wisconsin Department of Natural Resources (WDNR) “Wiscland 2 User Guide.” *Wiscland 2*, GIS Services Section, 2017, Madison, WI, Wisconsin Department of Natural Resources

Wisconsin Department of Natural Resources (WDNR). 2018a. Remedial Action Plan Update for the Lower Green Bay and Fox River Area of Concern, April 2018, Madison, WI, Wisconsin Department of Natural Resources.

Chapter 2: The Influence of Storm Trajectory, Antecedent Precipitation, and Seasonal Effects on Beryllium-7 and Excess Lead-210 Wet Deposition in the Upper Midwest, USA

Abstract

Depositional fluxes and concentrations of the fallout radionuclides (FRNs) beryllium -7 (^{7}Be) and excess lead-210 ($^{210}Pb_{xs}$) are assumed to be reasonably well-correlated in many sediment tracing and aging studies that employ these nuclides. However, growing evidence suggests the depositional patterns of these FRNs vary with numerous environmental conditions. I expanded on these findings by using the Hybrid Single-Particle Lagrangian Integrated Trajectory (HYSPLIT) model to trace the back trajectories for individual storm events and storm series for which the ^{7}Be and $^{210}Pb_{xs}$ activities of precipitation were measured at sites in the Upper Midwest, USA during 2016-2019. Average FRN ratios changed seasonally in the order of spring >winter >summer>fall. Measured depositional fluxes ranged from 0.0 $Bq \cdot m^{-2}$ to 144.5 $Bq \cdot m^{-2}$ for $^{210}Pb_{xs}$ and from 0.0 to 936.6 $Bq \cdot m^{-2}$ for ^{7}Be. Depositional fluxes correlated with precipitation totals. Seasonal depositional flux averages for both FRNs changed in the order of spring > summer > fall > winter. ^{7}Be and $^{210}Pb_{xs}$ depositional fluxes were found to vary by airmass trajectories in all seasons. Trajectories may have influenced FRN depositional fluxes by being associated with certain storm characteristics or by passing over regions with high concentrations of FRNs available for scavenging.

Introduction

The depositional patterns and chemical properties of the fallout radionuclides (FRNs) beryllium-7 (^{7}Be) and lead-210 (^{210}Pb) have made them useful together as

tracers of surface particles and aerosols (Koch et al., 1996; Matisoff et al., 2005; Wilson et al.,2008). ^{7}Be ($t_{1/2}$ =53.12 days) and ^{210}Pb ($t_{1/2}$ = 22.3 years) both bind strongly and irreversibly to fine particles and aerosols under various environmental conditions, facilitating their use as tracers (Pawlowski & Karwan, 2019; Landis et al., 2021). ^{7}Be is generated in the stratosphere and upper troposphere by the spallation of nitrogen and oxygen while ^{210}Pb is a product of the uranium-238 decay chain, entering the atmosphere near the surface by the decay of geogenic radon-222 gas (Sykora and Froehlich, 2009). A portion of ^{210}Pb remains in equilibrium with radium-226 in the subsurface and is considered "supported" ^{210}Pb. The other portion is deemed excess ^{210}Pb ($^{210}Pb_{xs}$) and is produced in the atmosphere after its parent isotope ^{222}Rn diffuses from the surface (Benmansour et al., 2014) . Wet deposition (e.g., rain and snow) mainly removes both radionuclides from the atmosphere (Calliet et al., 2001). A primary assumption in studies that use ^{7}Be and $^{210}Pb_{xs}$ together as tracers is that they are deposited in roughly equal ratios in precipitation (Matisoff et al., 2005). In many cases, both wash from the atmosphere in highly correlative concentrations such that their ratio to one another in precipitation is more consistent than the concentration of either FRN alone (Todd et al.,1989; Calliet et al.,2001).

While the correlation between ^{7}Be and $^{210}Pb_{xs}$ deposition is generally strong, their ratio in precipitation varies under different conditions. ^{7}Be production corresponds with a cycle of sunspot occurrence that lasts approximately eleven years and affects cosmic ray spallation in the atmosphere (Al-Azmi et al., 2001). The lower height of the tropopause at higher latitudes allows increased ^{7}Be scavenging in these regions (Kaste et al., 2002). Seasonal effects also play large roles in controlling FRN deposition at many sites.

Depositional fluxes can vary seasonally due to atmospheric mixing processes, rainfall totals, predominant storm types, and geographic effects (Baskaran 1995; McNeary and Baskaran, 2003, Ioannidou et al., 2005; Du et al., 2015). A 12-year study of monthly depositional fluxes in Tatsunokuchi, Japan observed that ^{7}Be and $^{210}Pb_{xs}$ shared similar responses to seasonal changes. This phenomenon was attributed to a combination of regionally relevant seasonal processes such as winter monsoons, airmass flows from high latitudes, and mixing from convection clouds generated over the Japan Sea (Yamamoto et. al., 2006). Seasonal changes in FRN deposition have been observed at several midlatitude sites (McNeary and Baskaran, 2003, Du et al., 2015), so I hypothesized that seasonal variation of FRN activities would be evident at sites in the Upper Midwest, USA, as well. At the storm event time scale, storm characteristics are important controls on FRN deposition. Storms with higher cloud-top heights tend to deposit greater concentrations of ^{7}Be due to the ability of tall clouds to scavenge ^{7}Be from the upper troposphere (Karwan et al., 2016). Precipitation type also affects FRN deposition as snow has been found to scavenge FRNs less efficiently than rain (Ioannidou and Papastefanou, 2006). The FRN composition of precipitation is further determined by storm intensity and duration (Renfro et al.,2013; Karwan et al., 2016), so I expected antecedent precipitation to be a control of FRN fluxes and concentrations in precipitation at the sites in this study. FRN concentrations in precipitation have been shown to decrease with storm duration and intensity due to atmospheric washout (Calliet et al., 2001). A time lag between deposition and atmospheric recharge results in low FRN activities measured after large precipitation events. ^{7}Be and $^{210}Pb_{xs}$ depositional fluxes have been found to be primarily

controlled by total rainfall at several sites when bulk precipitation was measured from days to months (Baskaran, 1995; Kaste et al., 2002; Calliet et al, 2005)

Less is known about how storm trajectories impact ^{7}Be and $^{210}Pb_{xs}$ wet deposition. So far, studies converge on observations of FRN deposition relating to distance from oceanic sources and latitudinal effects. It has been shown that $^{210}Pb_{xs}$ is depleted in maritime airmasses due to the absence of ^{222}Rn outgassing over oceans, affecting the availability of the daughter nuclide $^{210}Pb_{xs}$ in the atmosphere to be scavenged (Du et al., 2015; Landis et al., 2021). While there are no nearby oceans at the sites studied in this project, variations in ^{222}Rn outgassing over the landscape exist (Zhang et al., 2021) and may affect $^{210}Pb_{xs}$ deposition if storms pass over regions with different ^{222}Rn outgassing potential. There is also evidence of variation in FRN deposition at different latitudes, with depositional fluxes of ^{7}Be increasing with distance from the equator (Du et al., 2015). Thus, it may be hypothesized that storms from higher latitudes produce grater ^{7}Be fluxes in precipitation. I seek to expand on these findings by observing the effects of airmass trajectories on ^{7}Be and $^{210}Pb_{xs}$ depositional trends at several mid-latitude, mid-continental sites in the Upper Midwest, USA.

Methods:

Figure 1: Map of precipitation sampling locations in the Upper Midwest, USA. Site One- Saint Paul, MN (n=108). Site Two- Minneapolis, MN (n=17). Site Three- Marcell Experimental Forest, MN (n=17). Site Four near Wrightstown, WI (n=15). Site 5- near Harlan, IN (n=4). n is the number of samples collected at each site over the duration of the study.

Fallout radionuclide activities of bulk precipitation samples were measured at five sites in the Upper Midwest from 2016-2019 across all seasons. Precipitation samples were collected in eight-inch diameter funnels feeding one-liter bottles. Both were washed in 5% HCl baths prior to collection to eliminate FRN sorption to the collection containers. Precipitation was sampled on an event basis after at least 0.12 inches of rain accumulated in collectors. Total daily precipitation data were retrieved from permanent and semi-permanent rain gauges near each site. FRNs were extracted from precipitation samples following the protocol of Karwan et al., 2016. Final FRN activities were adjusted to account for recovery on the ion exchange resins using ICP-MS readings of stable Be and Pb concentrations in exchange resin supernatant (Karwan et al., 2016). Precipitation

samples were then analyzed for ^{7}Be and $^{210}Pb_{xs}$ activity with a Canberra HPGe detector using methods from Karwan et al., 2016, 2018.

Back-trajectories were modeled for each event using the Hybrid Single-Particle Lagrangian Integrated Trajectory (HYSPLIT) model (Draxler et al., 1997; Draxler et al., 1998; Draxler et al., 1999; Rolf et al., 2017; Stein et al., 2015). Back-trajectories were modeled at three km and fifteen km to account for the differences in the atmospheric production of ^{7}Be and $^{210}Pb_{xs}$. I assumed the three km above mean sea level (AMSL) back-trajectory altitude would be more likely to associate with $^{210}Pb_{xs}$ deposition due to its production by geogenic outgassing of ^{222}Rn. We assumed a 15 km AMSL back-trajectory would most accurately depict the atmospheric path of ^{7}Be because of its production by spallation in the upper troposphere and stratosphere. Back-trajectory models were run for the 72 hours leading up to the last day of precipitation accumulation in each sampling period.

Results:

The site with a vast majority of precipitation samples measured for FRN activities was Site One with 108 of 161 total samples. Seventeen or less samples were taken from all four of the other sites. Measured ^{7}Be concentrations at all sites ranged from 0 to 21.3 (+/- 30) Bq· kg^{-1}, and $^{210}Pb_{xs}$ concentrations ranged from 0 to 4.10 (+/- 0.20) Bq· kg^{-1} (*Table 1*.)

Site	Range of ^{7}Be ($Bq \cdot kg^{-1}$)	Range of $^{210}Pb_{xs}$ ($Bq \cdot kg^{-1}$)	Number of samples
1	0 to 7.60 (±0.20)	0 to 4.10 (±0.20)	108
2	0 to 21.3 (±0.30)	0 to 3.30 (±0.02)	17
3	0 to 2.50 (±0.02)	0 to 0.92 (±0.30)	17
4	0 to 4.00 (±0.05)	0 to 0.79 (±0.05)	15
5	0.02 (± 0.002) to 2.34 (± 0.06)	0 to 0.98 (+/- 0.03)	4

Table 1: The ranges of ^{7}Be and $^{210}Pb_{xs}$ concentrations measured in precipitation at each site over the duration of the study.

The depositional fluxes of ^{7}Be and $^{210}Pb_{xs}$ varied by storm back-trajectory and season (Figs. 1a & 1b).

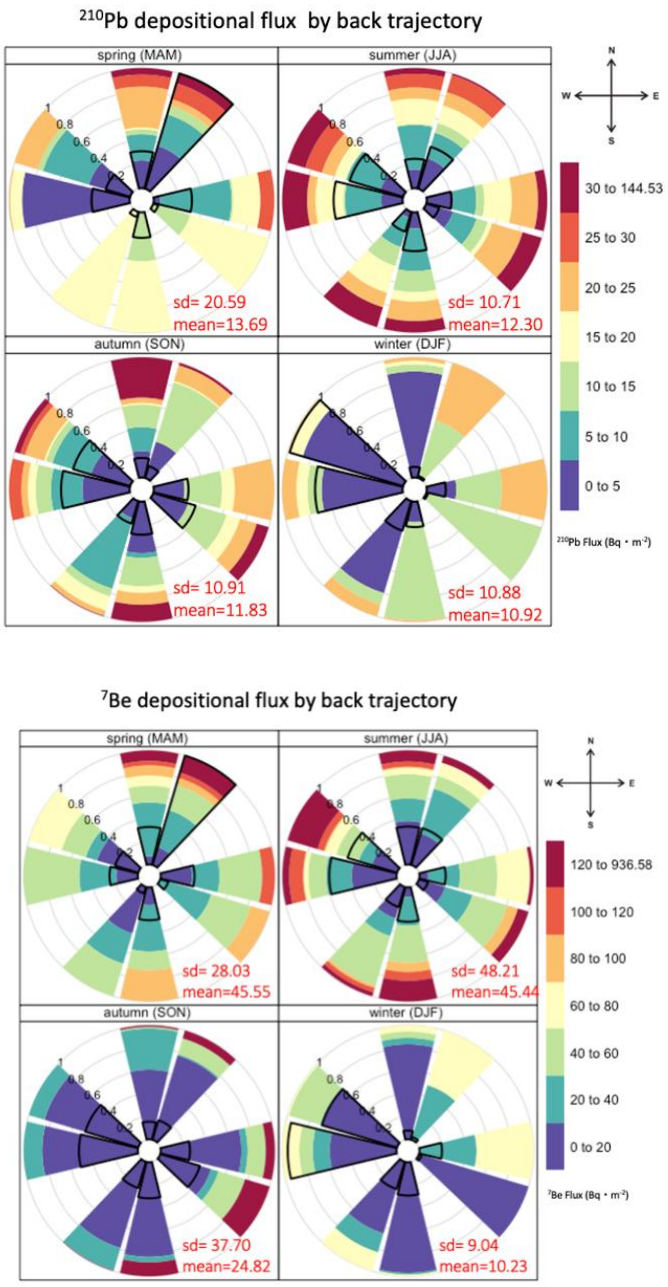

Figure 2a (top): $^{210}Pb_{xs}$ depositional flux by storm back-trajectory for each sampling site and date at 15 km above mean sea level. *Figure 2b (Bottom)*: ^{7}Be depositional flux in precipitation by storm back-trajectory for each sampling site and date at 3 km above mean sea level. Both figures reflect precipitation data from all five sites. The position of each bar indicates the cardinal direction that sampled storms derived from. 72-hour back-

trajectories starting on the last day of wet deposition before each collection date were calculated and split into 8 directional sectors by HYSPLIT. Colors indicate the proportion of storms from each trajectory sector with a particular range of flux values. The standard deviations and means of fluxes are printed for each season.

The most common back-trajectory of sampled storms in spring was northeast, as seen by the black outline in *Fig.2a*. Storms from the northeast also most frequently yielded the highest ^{7}Be fluxes (120 to 938.58 $Bq \cdot m^{-2}$). Storms from the north and northeast most frequently resulted in the highest $^{210}Pb_{xs}$ fluxes in the same period. During the summer, the back-trajectories of sampled storms were more evenly distributed in all directions. Summer storms most frequently producing the highest ^{7}Be fluxes came from the northwest and south. Summer storms frequently produced high $^{210}Pb_{xs}$ fluxes (25-144.53 $Bq \cdot m^{-2}$) whether they came from any direction. In autumn, storms from the southeast most frequently yielded the highest ^{7}Be fluxes, and storms from the north most often resulted in the highest $^{210}Pb_{xs}$ fluxes. In winter, storms from the east and northeast most frequently produced the highest ^{7}Be and $^{210}Pb_{xs}$ fluxes. Though, sampled storms in the winter were least likely to come from these directions. Winter storms from the northwest were the most frequent for the season, and they also had the lowest $^{210}Pb_{xs}$ depositional fluxes.

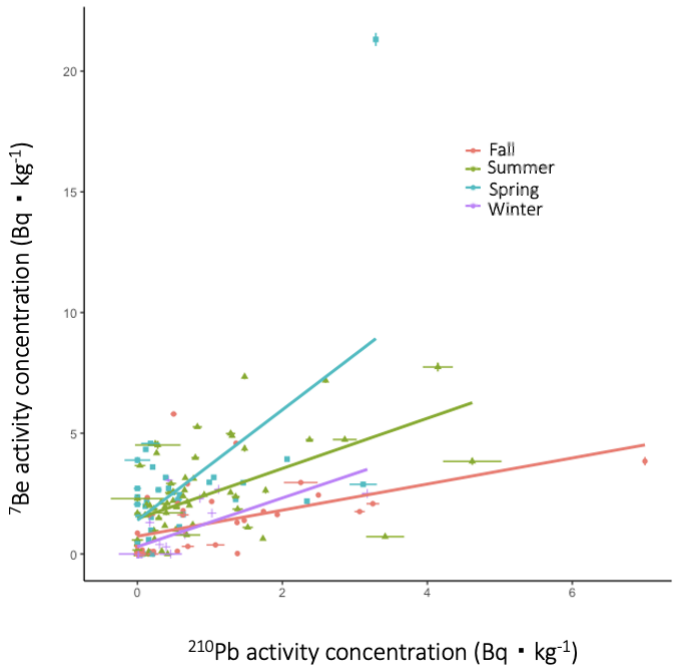

Figure 3: ^{7}Be vs $^{210}Pb_{xs}$ concentration relationships among all rain samples (snow excluded) and sites.

The slope of the ^{7}Be vs $^{210}Pb_{xs}$ linear regression in precipitation decreases in the order of spring >winter >summer>fall (*Fig. 3*). Though, the high regression slope for the winter months could be an artifact of a small sample size. The concentration regressions showed significant (p-value < 0.01) positive linear relationships across all seasons. Regression slopes were less than one for fall, winter, and summer, indicating that small increases in $^{210}Pb_{xs}$ concentrations corresponded with relatively large increases in ^{7}Be concentrations.

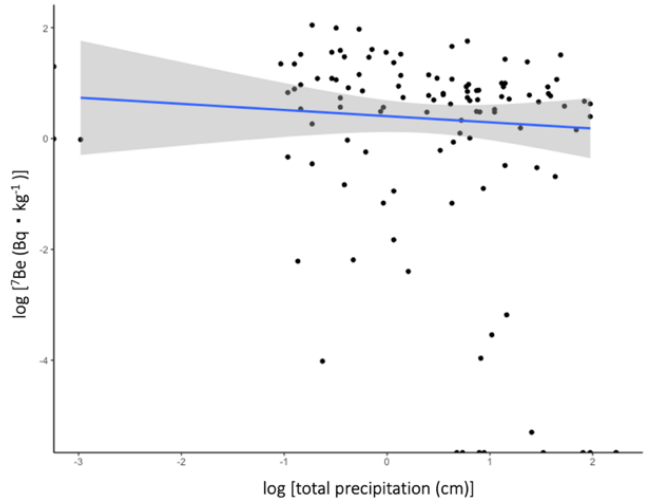
log [^{7}Be (Bq • kg^{-1})]
log [total precipitation (cm)]

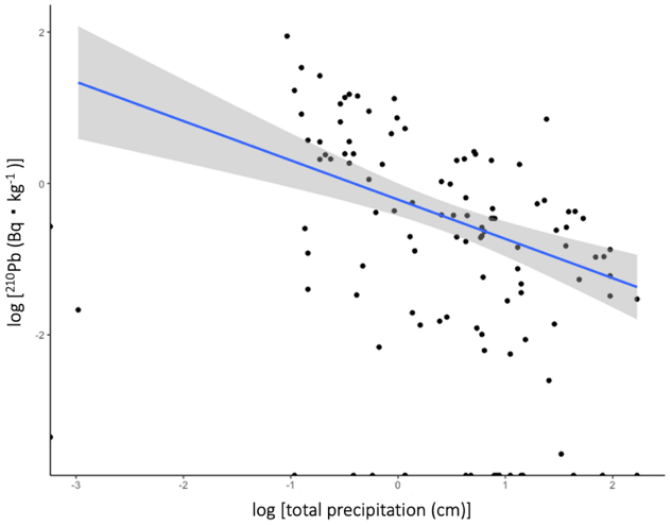
log [^{210}Pb (Bq • kg^{-1})]
log [total precipitation (cm)]

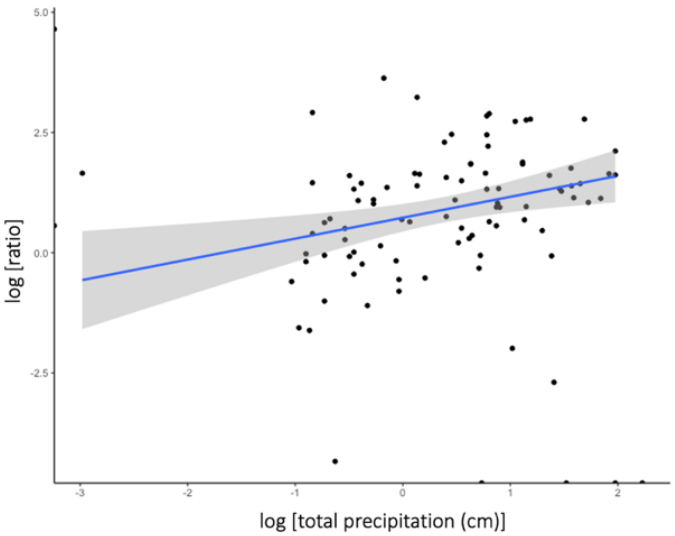
log [ratio]
log [total precipitation (cm)]

Figures 4a, 4b, & 4c (top to bottom): logarithmic regressions of FRN activity concentrations and $^{7}Be/^{210}Pb_{xs}$ ratio versus the total precipitation over each sampling period. The shaded gray area represents the standard error.

Fig. 4a shows a slightly negative log relationship between ^{7}Be activity concentration and total precipitation. *Fig. 4b* reveals a stronger negative log relationship between the $^{210}Pb_{xs}$ activity concentration and precipitation. For both ^{7}Be and $^{210}Pb_{xs}$, there is a high spread of FRN activities when precipitation totals are low. The spread of values decreases with increased precipitation totals, and activity values lower with increased precipitation. The standard error for the FRN concentrations was greatest at low total rainfall. As displayed in *Fig. 4c*, there is a positive linear log relationship between the $^{7}Be/^{210}Pb_{xs}$ ratio and precipitation totals, driven by the negative log relationship between $^{210}Pb_{xs}$ and total precipitation.

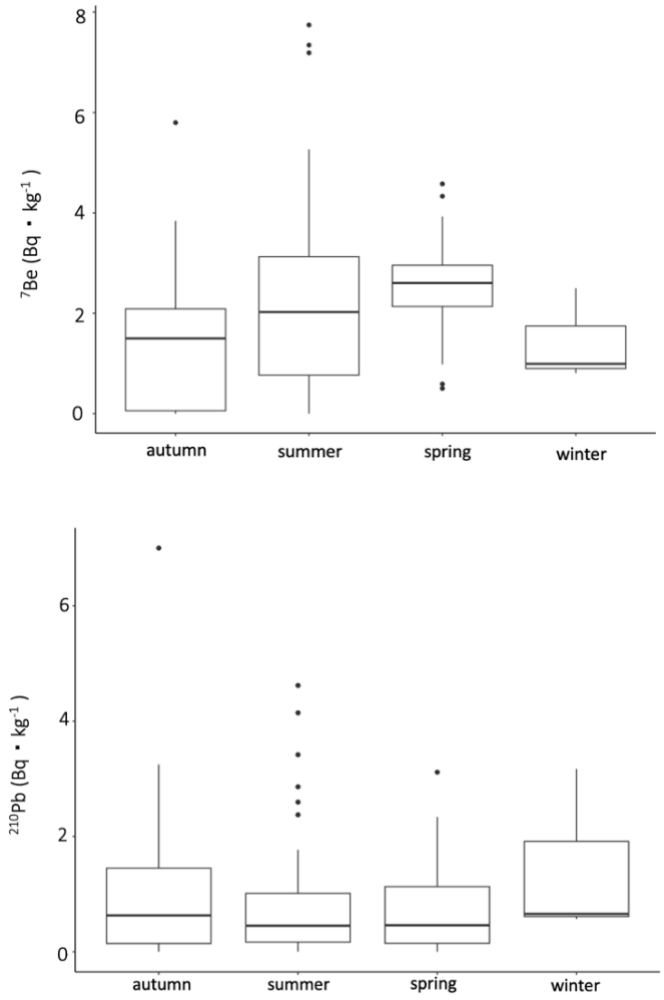

Figs 5a & 5b: FRN activity concentrations in rain across seasons and sampling locations.

The ^{7}Be activity concentrations in rain showed slightly higher concentrations in spring and summer than in fall and winter (*Fig. 5a*). Summer had the highest spread of ^{7}Be values from 0 to 7.74 Bq · kg^{-1} and had an average of 2.287 Bq · kg^{-1}. Winter had the smallest spread of ^{7}Be concentrations from 0 to 2.50 Bq · kg^{-1} and the lowest mean ^{7}Be concentration of 1.43 Bq · kg^{-1}. In spring, ^{7}Be concentrations in rain ranged from 0.50 to 4.58 Bq · kg^{-1} and averaged 2.51 Bq · kg^{-1}. Fall had an average ^{7}Be concentration of 1.39 Bq · kg^{-1} and a range of 0 to 5.79 Bq · kg^{-1}. The spread of $^{210}Pb_{xs}$ activity

concentrations were virtually equal across seasons, with slightly higher means and upper quantiles in winter and fall than in summer and spring (*Fig. 5b*). $^{210}Pb_{xs}$ activities were an average of 1.09 Bq · kg^{-1} in fall, 0.79 Bq · kg^{-1} in summer, 0.78 Bq · kg^{-1} in spring, and 1.47 Bq · kg^{-1} in winter.

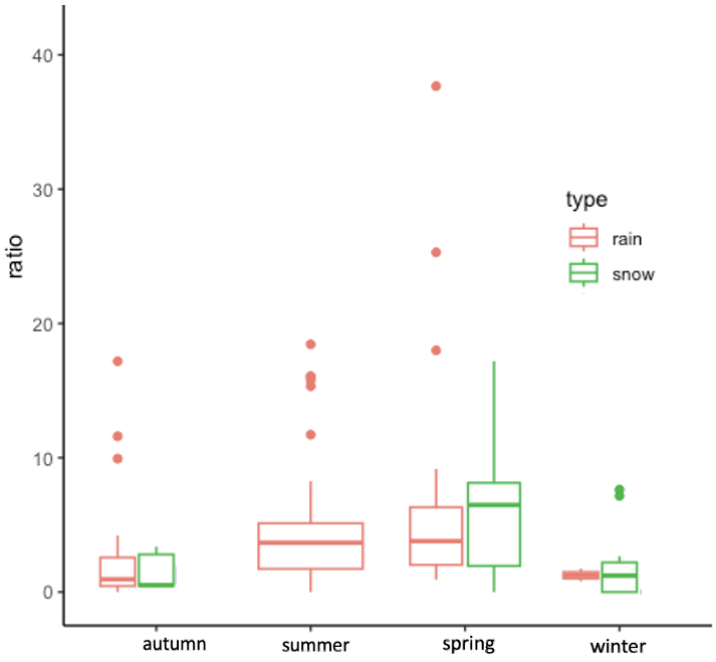

Figure 6: $^{7}Be/^{210}Pb_{xs}$ activity ratios in rain and snow are compared across all seasons.

Snow and rain had relatively equal ratios in the fall and winter while the mean and upper two quantiles of snow ratios exceeded those of rain during the spring (*Fig. 6*).

Discussion:

The fluxes of both ^{7}Be and $^{210}Pb_{xs}$ were shown to vary by storm back-trajectory and season. Different trajectories yielded the highest FRN fluxes in different seasons. A notable shift in trajectories associated with high ^{7}Be fluxes occurs between summer and fall. In summer, the highest ^{7}Be depositional fluxes tend to come from the northwest, west, and south. In fall, the highest fluxes came from the east (southeast, east,

northeast) while western trajectories (northwest, west, southwest) tended to produce lower fluxes. The variation of ^{7}Be depositional fluxes with trajectory and season disagreed with the original hypothesis that northern trajectories would produce higher fluxes. This was true in some, but not all months. I expected northern trajectories to yield higher ^{7}Be fluxes because of the lower tropopause at higher latitudes that has been thought to allow airmasses to better scavenge ^{7}Be (Kaste et al., 2002). The effect of airmass origination and seasonality on FRN fluxes may be explained by several interacting factors. Dominant storm types may be associated with different trajectories, affecting scavenging and deposition. Karwan et al. (2018) found that storm synoptic classification related to ^{7}Be and $^{210}Pb_{xs}$ depositional fluxes. Furthermore, this and other studies have found that depositional fluxes for both ^{7}Be and $^{210}Pb_{xs}$ correlate with high precipitation totals (Lozano et al., 2011; Pham et al.,2013; Mohan et al., 2019). Su et al. (2006) found that ^{7}Be and $^{210}Pb_{xs}$ concentrations in cloud water were affected by airmass sources that related to different storm types. If precipitation-intense storms are more likely to come from the northwest and south in the summer, storms from these directions may produce greater ^{7}Be fluxes in general. In the winter, more intense storms may be more likely to come from the northeast and east. $^{210}Pb_{xs}$ fluxes also varied by back-trajectory and season. In the summer, there was a relatively consistent distribution of high $^{210}Pb_{xs}$ flux storms from all directions. This contrasts with the spring, where high fluxes were associated with northern trajectories (north, northwest, northeast), and low fluxes tended to come from the south. It is possible that north-derived spring storms deposit more precipitation, and thus yield higher FRN fluxes. Previous work has shown that storm track variations in winter correspond with extreme precipitation events (Cheng-

Geng & Chang, 2017), but more work is needed to explore the relationships between precipitation intensity and storm trajectories across seasons to explain FRN fluxes. Another explanation for the difference in $^{210}Pb_{xs}$ fluxes in the spring and summer could be differences in regional ^{222}Rn outgassing that become more prevalent in the winter and early spring as ^{222}Rn emissions fluxes decrease in North America (Zhang et al., 2021). The low $^{210}Pb_{xs}$ fluxes measured in winter during this study (*Fig. 2a*) could reflect the decrease in ^{222}Rn outgassing that occurs in the same season (Zhang et al., 2021).

Precipitation type was another influence on FRN ratios. The results of this study agree with previous work that has shown that snow less efficiently scavenges ^{7}Be than rain (Kim et al., 1999). Snow had lower average ^{7}Be and $^{210}Pb_{xs}$ concentrations than rain across all seasons. The higher average FRN ratio of snow than rain in spring was influenced by the very low seasonal average $^{210}Pb_{xs}$ concentrations ($0.47\ Bq \cdot kg^{-1}$) in snow. While higher FRN ratios were evident in snow compared to rain in spring, differences in FRN ratios between precipitation types were negligible in the fall and winter.

Antecedent precipitation proved to strongly affect FRN fluxes, as hypothesized. As antecedent precipitation increased, fluxes decreased, and the spread of fluxes decreased for both FRNs. These findings agreed well with similar studies that attribute this phenomenon to atmospheric washout (McNeary and Baskaran, 2003; Pham et al., 2013). $^{210}Pb_{xs}$ fluxes were more strongly affected by precipitation totals over each sampling period than ^{7}Be fluxes. This can be explained by the ability of ^{7}Be to recharge more quickly than $^{210}Pb_{xs}$ at midlatitudes when there is vertical atmospheric mixing and a preference for cyclone formation, a process described by Landis et al. (2021) as synoptic

atmospheric recharge. These conditions exist during storm events with heavy rainfall, causing ^{7}Be recharge to occur quickly relative to that of $^{210}Pb_{xs}$ (Landis et al., 2021). With intense or persistent rain events, ^{7}Be is deposited in relatively consistent concentrations while $^{210}Pb_{xs}$ sees concentrations lower over the same period. Thus, the $^{7}Be/^{210}Pb_{xs}$ ratio increases with increased precipitation over individual and back-to-back storm events, as evidenced by Fig.6. Similar increases in the $^{7}Be/^{210}Pb_{xs}$ activity of precipitation were recorded over successive monsoons in Laos by Gourdin et al., 2014.

The $^{7}Be/^{210}Pb_{xs}$ activity ratios in precipitation were also affected by seasonal changes, agreeing with the original hypothesis. ^{7}Be showed stronger seasonal dependence than $^{210}Pb_{xs}$ (Figs. 7 & 8). In the spring and summer, FRN ratios in precipitation were higher because ^{7}Be concentrations increased relative to fall and winter. The increase in ^{7}Be concentrations in precipitation in the spring and summer is likely due to greater stratosphere-troposphere exchange in spring and large-scale atmospheric mixing in the summer that facilitate ^{7}Be scavenging by clouds (Dueñas et al.,2001; McNeary & Baskaran, 2003). In the winter, ^{7}Be deposition is relatively lower than in other seasons, but $^{210}Pb_{xs}$ deposition generally stays about the same (Figs. 7 & 8). The relationship between ^{7}Be and $^{210}Pb_{xs}$ activity concentrations changes with the season (Fig. 3). The trend of ^{7}Be concentrations decreasing in the fall and winter while $^{210}Pb_{xs}$ concentrations stay about the same can result in extremely low FRN ratios in precipitation during these seasons. The consistent seasonal trend in $^{210}Pb_{xs}$ deposition differs from findings at other locations. Dueñas et al. (2005) measured wet deposition of $^{210}Pb_{xs}$ in coastal Spain and found that $^{210}Pb_{xs}$ concentrations in rain decreased in the winter months, unlike this study. Hirose et al. (2004) observed higher $^{210}Pb_{xs}$ concentrations in rainwater in the winter than

in other months at two locations in Japan. Thus, the seasonal behaviors of $^{210}Pb_{xs}$ deposition vary geographically. At the midcontinental North American sites analyzed in this study, geographically influenced factors such as ^{222}Rn outgassing potential on the landscape, as well as predominant storm characteristics, may each influence $^{210}Pb_{xs}$ deposition differently in Midwestern, USA sites than in other regions.

Future studies can improve upon this work by investigating how storm characteristics relate to storm trajectories in this region. Future works that investigate how storm types are related to storm trajectories and how each connects to depositional fluxes would help explain why different trajectories produce different fluxes and why this changes seasonally.

Conclusion

Various environmental conditions influence ^{7}Be and $^{210}Pb_{xs}$ depositional patterns. ^{7}Be and $^{210}Pb_{xs}$ deposition change based on the paths of storms. This may either be due to differences in the availability of FRNs to be scavenged by storms along certain routes, or it is possible that different storm trajectories produce storms with different characteristics that in turn influence FRN deposition. Antecedent precipitation and seasonal effects also proved to be strong controls on FRN deposition.

The combined influence of storm trajectories, antecedent precipitation, and seasonal effects on the makeup of $^{7}Be/^{210}Pb_{xs}$ ratios in wet deposition call into question the assumption of a consistent FRN ratio in wet deposition commonly held by those conducting tracer studies. In the first chapter of this thesis, I found that low FRN activities in precipitation in winter and late fall can result in $^{7}Be/^{210}Pb_{xs}$ ratios of

precipitation that are less than those of stream sediment. This phenomenon can cause false estimations of sediment age during these seasons. Future sediment aging work using these nuclides should incorporate robust precipitation sampling schemes to prevent misinterpretation of sediment ages and sources.

Works Cited

Al-Azmi, D., A. M. Sayed, and H. A. Yatim. "Variations in 7Be concentrations in the atmosphere of Kuwait during the period 1994 to 1998." Applied Radiation and Isotopes 55.3 (2001): 413-417.

Baskaran, M. "A search for the seasonal variability on the depositional fluxes of 7Be and 210Pb." *Journal of Geophysical Research: Atmospheres* 100.D2 (1995): 2833 2840.

Benmansour, M., et al. "The Use of Excess 210 Pb (210 Pbex) as A Soil and Sediment Tracer." IAEA TECDOC SERIES 79 (2014).

Caillet, Stéphane, et al. "Factors controlling 7Be and 210Pb atmospheric deposition as revealed by sampling individual rain events in the region of Geneva, Switzerland." *Journal of Environmental Radioactivity* 53.2 (2001): 241-256.

Ma, Chen-Geng, and Edmund KM Chang. "Impacts of storm-track variations on wintertime extreme weather events over the continental United States." Journal of Climate 30.12(2017):4601-4624.

Du, Juan, et al. "Temporal variations of atmospheric depositional fluxes of 7Be and 210Pb over 8 years (2006–2013) at Shanghai, China, and synthesis of global fallout data." *Journal of Geophysical Research: Atmospheres* 120.9 (2015): 4323-4339

Dueñas, C., et al. "Deposition velocities and washout ratios on a coastal site (southeastern Spain) calculated from 7Be and 210Pb measurements." Atmospheric Environment 39.36 (2005): 6897-6908.

Dueñas, C., et al. "Atmospheric deposition of 7Be at a coastal Mediterranean station." Journal of Geophysical Research: Atmospheres 106.D24 (2001): 34059-34065.

Gourdin, Elian, et al. "Spatial and temporal variability of 7Be and 210Pb wet deposition during four successive monsoon storms in a catchment of northern Laos." Journal of environmental radioactivity 136 (2014): 195-205.

Ioannidou, Alexandra, M. Manolopoulou, and C. Papastefanou. "Temporal changes of 7Be and 210Pb concentrations in surface air at temperate latitudes (40 N)." Applied Radiation and Isotopes 63.2 (2005): 277-284.

Ioannidou, Alexandra, and C. Papastefanou. "Precipitation scavenging of 7Be and 137Cs radionuclides in air." Journal of Environmental Radioactivity 85.1 (2006): 121 36.

Koch, Dorothy M., Daniel J. Jacob, and William C. Graustein. "Vertical transport of tropospheric aerosols as indicated by 7Be and 210Pb in a chemical tracer model." *Journal of Geophysical Research: Atmospheres* 101.D13 (1996): 18651 18666.

Landis, Joshua David, et al. "Patterns and Processes in Aerosol Bulk Deposition: Insights from a 9-year Study of 7Be, 210Pb, Sulfate and Major/Trace Elements." *Authorea Preprints* (2022).

Lozano, R. L., et al. "Depositional fluxes and concentrations of 7Be and 210Pb in bulk precipitation and aerosols at the interface of Atlantic and Mediterranean coasts in Spain."Journal of Geophysical Research: Atmospheres 116.D18 (2011).

McNeary, D., and M. Baskaran. "Depositional characteristics of 7Be and 210Pb in southeastern Michigan." *Journal of Geophysical Research: Atmospheres* 108.D7 (2003).

Mohan, M. P., et al. "Influence of rainfall on atmospheric deposition fluxes of 7Be and 210Pb in Mangaluru (Mangalore) at the Southwest Coast of India." Atmospheric Environment 202 (2019): 281-295.

Muñoz-Arcos, E., et al. "Understanding the complexity of sediment residence time in rivers: Application of Fallout Radionuclides (FRNs)." *Earth-Science Reviews* (2022): 104188.

Pham, Mai K., et al. "Dry and wet deposition of 7Be, 210Pb and 137Cs in Monaco air during 1998–2010: seasonal variations of deposition fluxes." Journal of environmental radioactivity 120 (2013): 45-57.

Renfro, Alisha A., J. Kirk Cochran, and Brian A. Colle. "Atmospheric fluxes of 7Be and 210Pb on monthly time-scales and during rainfall events at Stony Brook, New York (USA)." *Journal of environmental radioactivity* 116 (2013): 114-123.

Stein, A.F., Draxler, R.R, Rolph, G.D., Stunder, B.J.B., Cohen, M.D., and Ngan, F., (2015).NOAA's HYSPLIT atmospheric transport and dispersion modeling system, Bull. Amer. Meteor. Soc., 96, 2059-2077, http://dx.doi.org/10.1175/BAMS-D-14-00110.1

Su, Chih-Chieh, and Chih-An Huh. "Measurements of 7Be and 210Pb in cloudwaters: Toward a better understanding of aerosol transport and scavenging." Geophysical research letters 33.4 (2006).

Sykora, Ivan, and Klaus Froehlich. "Radionuclides as tracers of atmospheric processes." *Radioactivity in the Environment* 16 (2009): 51-88.

Todd, James F., et al. "Atmospheric depositional characteristics of beryllium 7 and lead 210 along the southeastern Virginia coast." *Journal of Geophysical Research: Atmospheres* 94.D8 (1989): 11106-11116.

Wilson, C. G., et al. "Quantifying relative contributions from sediment sources in Conservation Effects Assessment Project watersheds." *Journal of Soil and Water Conservation* 63.6 (2008): 523-532.

Yamamoto, Masayoshi, et al. "Seasonal and spatial variation of atmospheric 210Pb and 7Be deposition: features of the Japan Sea side of Japan." Journal of Environmental Radioactivity 86.1 (2006): 110-131.

Zhang, Bo, et al. "Simulation of radon-222 with the GEOS-Chem global model: \ emissions, seasonality, and convective transport." Atmospheric Chemistry and Physics 21.3 (2021): 1861-1887.